JACS
JOURNAL OF THE AMERICAN CHEMICAL SOCIETY

Article

pubs.acs.org/JACS

N–N Bond Cleavage of 1,2-Diarylhydrazines and N–H Bond Formation via H-Atom Transfer in Vanadium Complexes Supported by a Redox-Active Ligand

Carsten Milsmann, Scott P. Semproni, and Paul J. Chirik*

Department of Chemistry, Princeton University, Princeton, New Jersey 08544, United States

Supporting Information

ABSTRACT: Addition of stoichiometric quantities of 1,2-diarylhydrazines to the bis(imino)pyridine vanadium dinitrogen complex, $[\{(^{iPr}BPDI)V(THF)\}_2(\mu_2\text{-}N_2)]$ ($^{iPr}BPDI$ = 2,6-(2,6-*i*Pr$_2$-C$_6$H$_3$N=CPh)$_2$C$_5$H$_3$N), resulted in N–N bond cleavage to yield the corresponding vanadium bis(amido) derivatives, ($^{iPr}BPDI$)V(NH*Ar*)$_2$ (Ar = Ph, Tol). Spectroscopic, structural, and computational studies support an assignment as vanadium(III) complexes with chelate radical anions, [BPDI]$^{\bullet-}$. With excess 1,2-diarylhydrazine, formation of the bis(imino)pyridine vanadium imide amide compounds, ($^{iPr}BPDI$)V(NH*Ar*)N*Ar*, were observed along with the corresponding aryldiazene and aniline. A DFT-computed N–H bond dissociation free energy of 69.2 kcal/mol was obtained for ($^{iPr}BPDI$)V(NHPh)NPh, and interconversion between this compound and ($^{iPr}BPDI$)V(NHPh)$_2$ with (2,2,6,6-tetramethylpiperidin-1-yl)oxidanyl (TEMPO), 1,2-diphenylhydrazine, and xanthene experimentally bracketed this value between 67.1 and 73.3 kcal/mol. For ($^{iPr}BPDI$)V(NHPh)$_2$, the N–H BDFE was DFT-calculated to be 64.1 kcal/mol, consistent with experimental observations. Catalytic disproportionation of 1,2-diarylhydrazines promoted by ($^{iPr}BPDI$)V(NH*Ar*)N*Ar* was observed, and crossover experiments established exchange of anilide (but not imido) ligands in the presence of free hydrazine. These studies demonstrate the promising role of redox-active active ligands in promoting N–N bond cleavage with concomitant N–H bond formation and how the electronic properties of the metal–ligand combination influence N–H bond dissociation free energies and related hydrogen atom transfer processes.

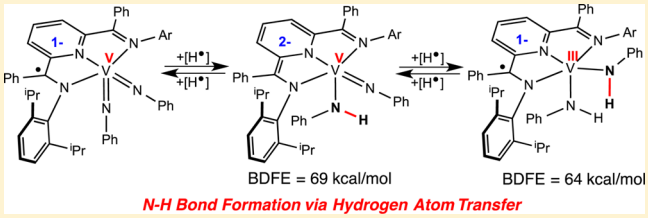

INTRODUCTION

Understanding the pathways for N–H bond formation with nitrogen-based ligands such as amides, hydrazides, imides, and nitrides in soluble coordination compounds is essential in the rational design of synthetic cycles for the functionalization of molecular nitrogen. In this context, stepwise proton-coupled electron transfer (PCET) has been firmly established as operative in both biological[1] and synthetic systems that catalytically form ammonia from N_2.[2] The special case of hydrogen atom transfer (HAT), in which the proton and electron move in a concerted step, has not been widely considered[3] or extensively studied for N–H bond formation. While hydrogen atom abstraction has been implied in a number of examples,[4] direct observation of HAT to metal imido complexes has only been observed in select cases.[5] Smith[6] and Hillhouse[7] have independently reported the application of both HAT and stepwise PCET for the interconversion of imido and amido complexes of iron, cobalt, and nickel and estimated thermodynamic parameters for N–H bond formation and cleavage.

Coupling N–N bond cleavage to N–H bond formation via HAT is attractive for N_2 functionalization but poses a fundamental challenge in coordination chemistry. Late metal imides are known to form strong N–H bonds via HAT,[8] a concept applied to important catalytic reactions such as the amination of unactivated C–H bonds,[9] but often lack the reduction potential to induce cleavage of strong N–N multiple bonds. On the other hand, early transition metal complexes are sufficiently reducing to promote N_2 cleavage[10] yet form strong metal–nitrogen bonds that are often inert to further functionalization chemistry.[11,12] Gaining a thorough understanding of the thermodynamic parameters associated with N–H bond formation via HAT, particularly in early transition metal complexes known to promote N–N cleavage, is therefore essential for rational design of soluble metal complexes for the synthesis of value-added nitrogen-containing compounds from N_2.

Reduced early transition metal complexes supported by redox-active ligands, those that can undergo reversible single electron transfer with a transition metal, are attractive for this purpose as the electronic flexibility imparted by the supporting ligand may, similar to cofactors in enzymatic catalysis, lower barriers for key bond cleavage and forming events.[13] Our laboratory recently demonstrated the application of this concept to the cleavage of the N=N double bond in azobenzene by the reduced bis(imino)pyridine vanadium dinitrogen complex $[\{(^{iPr}BPDI)V(THF)\}_2(\mu_2\text{-}N_2)]$ ($^{iPr}BPDI$ = 2,6-(2,6-*i*Pr$_2$-C$_6$H$_3$N=CPh)$_2$C$_5$H$_3$N).[14] By establishing the electronic structures of both $[\{(^{iPr}BPDI)V(THF)\}_2(\mu_2\text{-}N_2)]$

Received: June 20, 2014
Published: July 28, 2014

   dx.doi.org/10.1021/ja5062196 | J. Am. Chem. Soc. 2014, 136, 12099–12107

and the resulting bis(imido) complex (^{iPr}BPDI)V(NPh)$_2$, we were able to show that the overall four-electron process results from cooperative redox events involving both the transition metal and the redox-active ligands. This process, in conjunction with the observation that related bis(imino)pyridine iron complexes,[15] undergoes rare examples of complete hydrogenolysis of the metal−nitrogen bond upon exposure to 1 atm of H_2 at 23 °C,[16] suggested that this family of compounds may find application in N−H bond formation following N_2 cleavage. Further precedent has been provided by the work of Heyduk et al., who showed that tantalum imido complexes supported by redox-active [NNN] and [ONO] pincer ligands undergo facile PCET with 1,2-diphenylhydrazine and other weak hydrogen atom donors.[17]

Inspired by these observations, we sought to further investigate early transition metal bis(imino)pyridine complexes with the goal of enabling both N−N bond cleavage and N−H bond formation via HAT at a single metal center. Here we describe the successful demonstration of such a sequence with the N−N bond cleavage in hydrazines promoted by a bis(imino)pyridine vanadium complex. Interconversion of amido and imido ligands was also observed and established the potential utility of redox-active supporting ligands in concerted PCET reactions.

RESULTS AND DISCUSSION

Synthesis and Characterization of a Bis(anilido) Complex from N−N Single Bond Cleavage. Our studies into N−N bond cleavage commenced with the addition of 2 equiv of 1,2-diphenylhydrazine to a diethyl ether solution of [{(^{iPr}BPDI)V(THF)}$_2$(μ_2-N_2)] at 20 °C. This procedure yielded a dark red powder identified as bis(imino)pyridine vanadium bis(anilido) complex, (^{iPr}BPDI)V(NHPh)$_2$, in 67% yield (eq 1). The infrared spectrum recorded in a solid KBr matrix exhibits two diagnostic N−H stretches at 3305 and 3281 cm^{-1}, supporting net oxidative addition of the N−N single bond to the [(BPDI)V] fragment. Magnetic susceptibility measurements established an S = 1/2 ground state (μ_{eff} = 1.7 μ_B), which was corroborated by room temperature EPR experiments. The EPR spectrum of (^{iPr}BPDI)V(HNPh)$_2$ was recorded in toluene solution at 23 °C (Figure 1) and exhibits two distinct signals. The main eight-line feature of the spectrum was readily simulated using an isotropic g value of 1.958 and an isotropic hyperfine coupling constant, A_{iso}, of 208 MHz. The latter arises from interaction of the electron spin with the vanadium nucleus (^{51}V, I = 7/2, 100%). The line shape was successfully modeled assuming residual anisotropy due to slow tumbling motion of the molecules in solution on the time scale of the experiment. The significant deviation from the g value of the free electron (g_{el} = 2.0023) and the large vanadium hyperfine coupling constant indicate a predominantly vanadium-centered spin. A second, smaller eight-line signal in the spectrum is due to an unidentified vanadium impurity (<4%) and was readily reproduced in the simulation assuming values of g_{iso} = 1.995 and A_{iso} = 40 MHz.

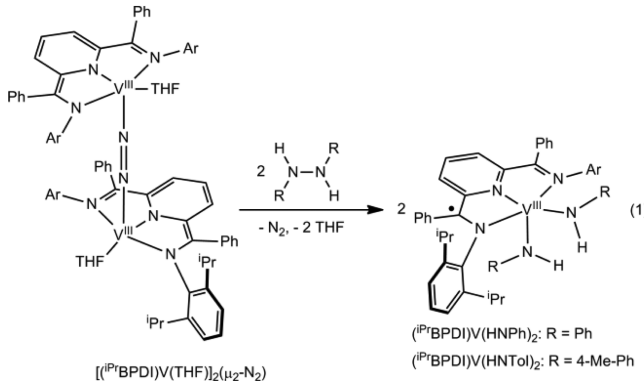

The tolyl-substituted analogue, (^{iPr}BPDI)V(HNTol)$_2$, was isolated in 58% yield following addition of 1,2-di-*p*-tolylhydrazine to the vanadium dinitrogen compound under identical reaction conditions (eq 1). The room temperature EPR spectrum in toluene solution is almost identical to the one reported for (^{iPr}BPDI)V(NHPh)$_2$ and was readily simulated using g_{iso} = 1.959 and A_{iso} = 206 MHz (see Supporting Information Figure S1). Single crystals suitable for X-ray diffraction were obtained from a pentane solution. The solid-state structure of (^{iPr}BPDI)V(HNTol)$_2$ is presented in Figure 2, and selected bond lengths and angles are reported in Table 1. The N−H protons were located in the difference map and freely refined, confirming formation of a vanadium bis(anilido) complex. This assignment is further supported by the relatively long V−N distances of 1.917(2) and 1.9009(18) Å as well as

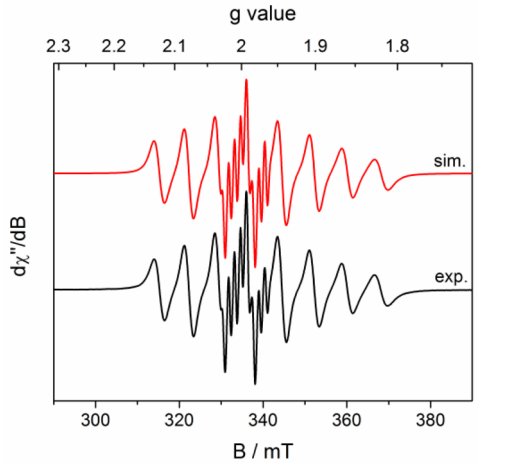

Figure 1. EPR spectrum of (^{iPr}BPDI)V(HNPh)$_2$ recorded at room temperature in toluene solution (microwave frequency = 9.374 GHz, power = 0.63 mW, modulation amplitude = 0.6 mT/100 kHz).

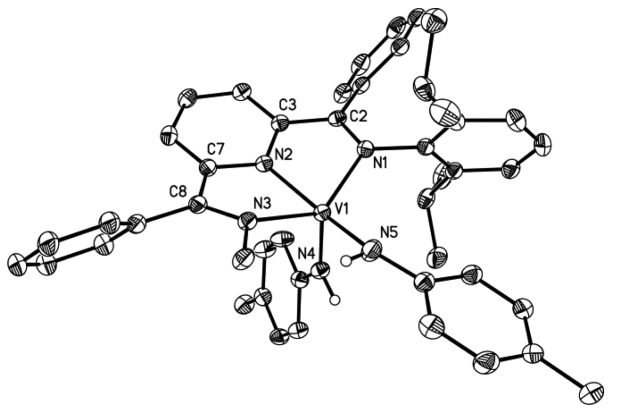

Figure 2. Representation of the molecular structure of (^{iPr}BPDI)V(HNTol)$_2$ with 30% probability ellipsoids. Hydrogens, except those on the anilido ligands, and one 2,6-di-isopropylphenyl substituent were omitted for clarity.

dx.doi.org/10.1021/ja5062196 | J. Am. Chem. Soc. 2014, 136, 12099−12107

Table 1. Selected Bond Distances (Å) and Angles (deg) for (^{iPr}BPDI)V(NPh)$_2$, (^{iPr}BPDI)V(NPh)(HNPh), and (^{iPr}BPDI)V(HNTol)$_2$

	(^{iPr}BPDI)V(NPh)$_2$[a]	(^{iPr}BPDI)V(NPh)(HNPh)	(^{iPr}BPDI)V(HNTol)$_2$
V(1)−N(1)	2.1457(16)	2.0366(17)	2.1131(17)
V(1)−N(2)	2.0569(16)	1.9988(17)	1.9812(17)
V(1)−N(3)	2.1623(15)	2.0934(17)	2.0495(16)
V(1)−N(4)	1.7108(16)	1.6999(16)	1.917(2)
V(1)−N(5)	1.6986(17)	1.9092(18)	1.9009(18)
N(1)−C(2)	1.329(3)	1.360(2)	1.334(3)
N(3)−C(8)	1.321(2)	1.340(2)	1.348(3)
N(2)−C(3)	1.367(3)	1.371(2)	1.380(3)
N(2)−C(7)	1.369(2)	1.375(2)	1.381(3)
C(2)−C(3)	1.438(3)	1.422(3)	1.430(3)
C(7)−C(8)	1.448(3)	1.428(3)	1.418(3)
V(1)−N(4)−C_{Ar}	171.47(14)	168.76(15)	147.16(19)
V(1)−N(5)−C_{Ar}	159.05(15)	138.61(14)	140.73(15)

[a]From ref 14.

the significantly bent V(1)−N(4)−C_{Ar} vectors of 147.16(19) and 140.73(15)° for the anilido ligands. By comparison, the geometric parameters of (^{iPr}BPDI)V(NPh)$_2$ with almost linear vanadium imido moieties are included in Table 1. It is now firmly established that the C_{im}−N_{im} and C_{im}−C_{ip} bond distances are indicative of the redox state of the bis(imino)-pyridine ligand framework and useful for assigning the redox state of the chelate.[18] The C_{im}−N_{im} bond distances of 1.334(3) and 1.348(3) Å in (^{iPr}BPDI)V(HNTol)$_2$ are slightly longer than those in (^{iPr}BPDI)V(NPh)$_2$, a compound established as having a one-electron reduced [BPDI]$^{\bullet-}$ radical ligand. These values are, however, significantly shorter than the corresponding bond lengths in [{(^{iPr}BPDI)V(THF)}$_2$(μ_2-N_2)] containing doubly reduced closed-shell [BPDI]$^{2-}$ ligands. To resolve this ambiguity and provide deeper insight into the oxidation states of both ligand and metal center, full-molecule DFT calculations were conducted at the B3LYP level. Assuming the experimentally determined S = 1/2 ground state, the calculations converged to a broken-symmetry (2,1) solution with spontaneous symmetry breaking. The optimized geometry (for coordinates, see Supporting Information) is in excellent agreement with the experimental data established by crystallography. The computed Mulliken spin density for (^{iPr}BPDI)V(HNPh)$_2$ is shown in Figure 3. The combined analyses of the DFT-computed orbital manifold and the spin population suggest that the complex is best described as V^{III} (d^2) with two unpaired electrons on the metal center antiferromagnetically coupled to a [BPDI]$^{\bullet-}$ radical anion. To provide additional support for the computational results, EPR parameters were calculated based on the obtained electronic structure, and the computed values of g_{iso} = 1.954 and A_{iso} = −172 MHz are in good agreement with the experimental data.

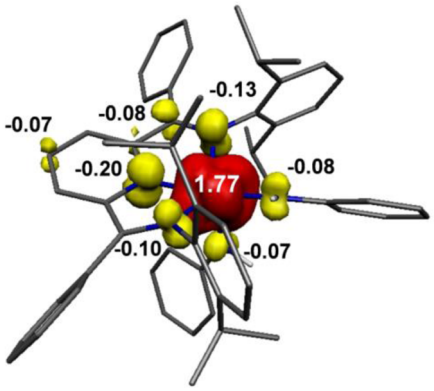

Figure 3. Spin density plot for (^{iPr}BPDI)V(HNPh)$_2$ obtained from Mulliken population analysis.

With the electronic structure of (^{iPr}BPDI)V(NH*Ar*)$_2$ established, the electron flow during the net two-electron, reductive N−N bond cleavage of 1,2-diarylhydrazines by [{(^{iPr}BPDI)V(THF)}$_2$(μ_2-N_2)] can be elucidated. In agreement with previous reports by Gambarotta and co-workers as well as our own independent structural data,[19] the starting dinitrogen compound is best described as a vanadium(III) complex with two-electron reduced chelates and a bridging $[N_2]^{2-}$ ligand. In contrast to the four-electron azo-N=N bond cleavage process, in which the electrons are supplied by the metal center, the supporting bis(imino)pyridine and the bridging N_2 ligand, the two electrons required for the N−N bond cleavage of hydrazine, are supplied exclusively by the ligands. The oxidation state of the bis(imino)pyridine ligand changes from [BPDI]$^{2-}$ in the starting material to [BPDI]$^{\bullet-}$ in the bis(anilido) vanadium product, providing one electron, while the $[N_2]^{2-}$ ligand supplies one electron to each [(BPDI)V] subunit, liberating a neutral dinitrogen molecule. Notably, the metal center maintains the +III oxidation state throughout the transformation.

Synthesis and Characterization of a Mixed Vanadium Imido/Anilido Complex. The net oxidative addition of 1,2-diarylhydrazines with [{(^{iPr}BPDI)V(THF)}$_2$(μ_2-N_2)] proceeded readily at room temperature without significant formation of observable byproducts. However, monitoring the addition of a large excess (~10 equiv) of 1,2-diphenylhydrazine to a benzene-d_6 solution of [{(^{iPr}BPDI)V(THF)}$_2$(μ_2-N_2)] by ^{1}H NMR spectroscopy and heating to 80 °C for 72 h yielded a new diamagnetic product in 72% yield as judged by integration against an internal ferrocene standard. Furthermore, 1.1 equiv of azobenzene and 3.3 equiv of aniline were detected in the reaction mixture with respect to vanadium in the starting material. Continued heating for an additional 48 h did not

dx.doi.org/10.1021/ja5062196 | J. Am. Chem. Soc. 2014, 136, 12099−12107

increase the yield of the diamagnetic product but resulted in complete consumption of hydrazine and increased the amount of azobenzene and aniline formed. The ^{1}H NMR spectrum of the vanadium product exhibits the number of resonances consistent with a C_s-symmetric compound. A singlet was located at 10.11 ppm, corresponding to a single proton without coupling to any carbon nucleus, as determined by ^{1}H−^{13}C NMR correlation experiments, and was assigned as an N−H resonance. Corroboration for this assignment was provided by observation of a band centered at 3334 cm^{-1} in the solid-state infrared spectrum. The combined spectroscopic data supported formation of the bis(imino)pyridine vanadium imido−amido complex, (^{iPr}BPDI)V(NPh)(HNPh), in the presence of excess hydrazine.

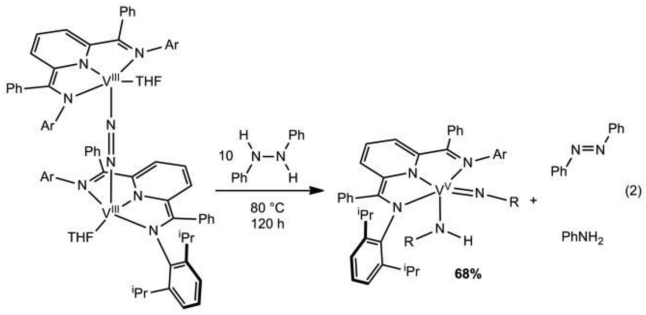

The solid-state structure of (^{iPr}BPDI)V(NPh)(HNPh) was determined by X-ray diffraction, and a representation of the molecule is shown in Figure 4. Selected bond distances and

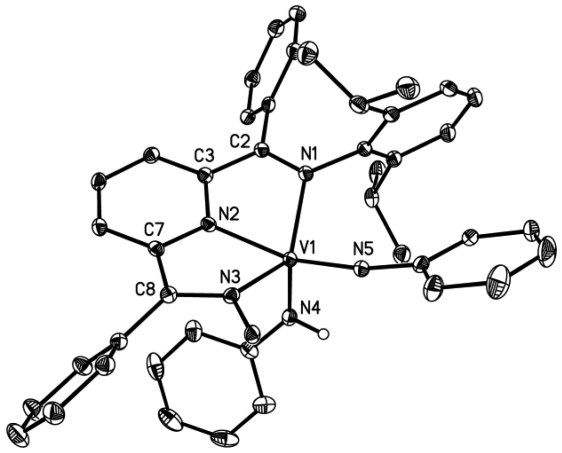

Figure 4. Representation of the molecular structure of (^{iPr}BPDI)V(NPh)(HNPh) with 30% probability ellipsoids. Hydrogens, except those on the anilido ligand, and one 2,6-di-isopropylphenyl substituent were omitted for clarity.

angles are reported in Table 1. The imido and anilido ligands are clearly distinguishable crystallographically, where the imido ligand occupies the basal position and is nearly linear (V(1)−N(5)−C_{Ar} = 168.76(15)°) with a short V−N bond length of 1.6999(16) Å, similar to the parameters observed in the bis(imido) complex (^{iPr}BPDI)V(NPh)$_2$.[14] In contrast, the apical anilido ligand displays a smaller V−N−C angle of 138.61(14)° and a longer metal ligand distance of 1.9092(18) Å. resembling the values in (^{iPr}BPDI)V(HNTol)$_2$. As in the bis(anilido) complex, the N−H proton of the anilido ligand was located in the difference map and freely refined. The preference for the isomer with the stronger *trans*-influence imido ligand in the basal position is unusual and may be a result of the redox-active ligand altering the electronic properties of the metal and hence coordination geometry. Additional experimental and computational studies are required to uncover the origin of this behavior. The structural parameters of the bis(imino)pyridine framework clearly indicate two-electron reduction of the ligand with elongated C_{im}−N_{im} and short C_{im}−C_{ip} distances. In agreement with computational results (see Supporting Information), the compound is, therefore, best described as a V^V complex with a closed-shell dianionic $[BPDI]^{2-}$ ligand.

Role of the Redox-Active Ligand during Hydrogen Atom Transfer. The determination of the electronic structures of (^{iPr}BPDI)V(N*Ar*)$_2$, (^{iPr}BPDI)V(NH*Ar*)(N*Ar*), and (^{iPr}BPDI)V(NH*Ar*)$_2$ highlights the ability of the redox-active ligand framework to adjust to the electronic requirements of the metal center during chemical transformations (Scheme 1). In (^{iPr}BPDI)V(NPh)$_2$, the two strongly π-donating imido ligands enable the formation of a reduced ligand radical anion, allowing the metal to remain in the +V (d^0) oxidation state. Note that the bond order of each imido ligand can be considered as 2.5; both the basal and apical imido ligands can form one full two-center two-electron π-bond with the metal center through the d_{xy} and d_{yz} orbitals, respectively; a second interaction through the d_{xz} orbital leads to the formation of a three-center four-electron bond. The addition of one hydrogen atom results in the formation of a new N−H bond in (^{iPr}BPDI)V(NPh)(HNPh), removing one possible π-interaction between the metal and the newly formed anilido ligand. This results in a strengthening of the V−N bond of the remaining basal imido ligand as indicated by the shorter V−N bond distance as compared to the bis(imido) complex. However, the total number of π-bonds formed by the vanadium center remains constant. Consequently, the additional electron supplied by the incoming hydrogen atom is relayed to the supporting redox-active ligand, allowing the metal to retain its high oxidation state. Upon further HAT to generate (^{iPr}BPDI)V(HNPh)$_2$, a second π-interaction is disrupted, rendering the vanadium ion more electropositive. As a result, the incoming electron is stored on the metal center and an additional reducing equivalent is transferred from the bis(imino)pyridine ligand, resulting in a doubly reduced V^{III} center and a one-electron oxidation of the chelating ligand.

Estimation of N−H Bond Dissociation Free Energies. The isolation and characterization of a series of related bis(imido), imido/anilido, and bis(anilido) vanadium complexes supported by the same redox-active bis(imino)pyridine ligand provides a rare opportunity to investigate HAT reactions relevant to N−H bond formation. Additional experimental and computational studies were conducted to determine the bond dissociation free energies (BDFEs) of the N−H bonds. A variety of different organic hydrogen atom donors with known H−E BDFEs was employed to investigate the feasibility of HAT for the synthesis of (^{iPr}BPDI)V(NH*Ar*)(N*Ar*) from (^{iPr}BPDI)V(N*Ar*)$_2$ and provide an experimental estimate for the resulting N−H bond strength. For consistency and ease of comparison, all BDFEs of the hydrogen atom donors used in this study are those reported in DMSO solution, and it is assumed that these values remain constant in THF, toluene, and benzene-d_6, the reaction media of the present chemistry.[20]

Addition of 1 equiv of TEMPO-H (BDFE(O−H) = 67.5 kcal/mol) to (^{iPr}BPDI)V(NPh)$_2$ resulted in clean conversion to the desired (^{iPr}BPDI)V(NH*Ar*)(N*Ar*) product immediately upon mixing in hydrocarbon or ethereal solvents. The formation of TEMPO radical as well as complete consumption

dx.doi.org/10.1021/ja5062196 | J. Am. Chem. Soc. 2014, 136, 12099−12107

Scheme 1. Summary of Bond Dissociation Free Energies and Changes in Electronic Structure upon HAT

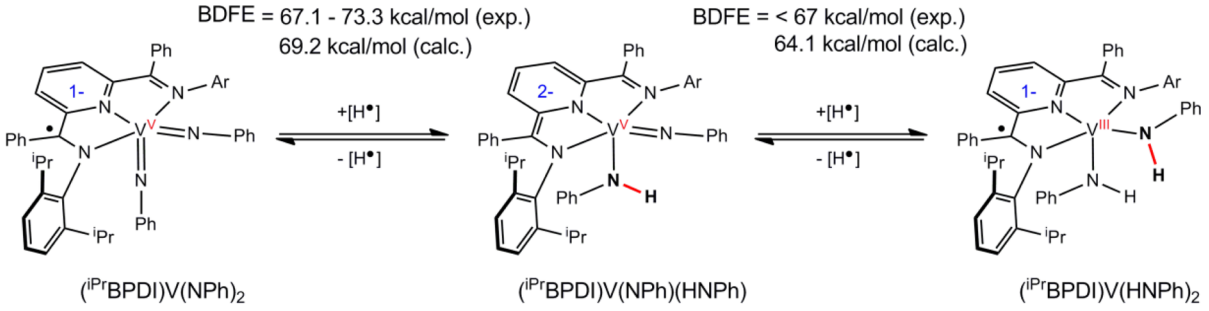

of the vanadium starting material was confirmed by EPR spectroscopy. Similarly, addition of 1,2-diphenylhydrazine (BDFE(N−H) = 67.1 kcal/mol) also proceeded cleanly and yielded the vanadium imido/anilido complex and azobenzene in the expected 2:1 ratio. In contrast, common hydrogen atom donors with slightly stronger E−H bonds such as xanthene (BDFE(C−H) = 73.3 kcal/mol) or 9,10-dihydroanthracene (DHA, BDFE(C−H) = 76.0 kcal/mol) proved unreactive, establishing that the BDFE of the anilido N−H bond in (^{iPr}BPDI)V(NPh)(HNPh) is in the range of 67.5−73.3 kcal/mol. We note that while the origin of this lack of reactivity is likely thermodynamic, kinetic barriers and polar components to the BDFEs cannot be rigorously excluded.

In an attempt to measure the BDFE of the N−H bonds in (^{iPr}BPDI)V(HNPh)$_2$, similar experiments were conducted by adding weak hydrogen atom donors to (^{iPr}BPDI)V(NPh)(HNPh). Even with the weakest donors, TEMPO-H or 1,2-diphenylhydrazine, no reaction was observed over extended periods, establishing a BDFE less than 67 kcal/mol. To confirm this value and exclude kinetic barriers for HAT, the reverse reaction was conducted. Addition of stoichiometric amounts of TEMPO to (^{iPr}BPDI)V(HNPh)$_2$ resulted in immediate formation of (^{iPr}BPDI)V(NPh)(HNPh) and TEMPO-H in the expected 1:1 ratio, supporting a thermodynamic and not kinetic barrier in the forward direction.

To support the experimental results, full-molecule, gas-phase DFT computations at the B3LYP level were conducted to obtain theoretical estimates of the N−H BDFEs. Note that the inclusion of the bulky 2,6-di-isopropylphenyl substituents was necessary, as the use of smaller model complexes led to complexes with trigonal bipyramidal structures in contrast to the experimentally observed square pyramidal geometries. DFT-computed BDFEs were obtained through numerical frequency analysis to include zero-point energy corrections and translational, rotational, and vibrational contributions to the Gibbs free energy at 298 K and 1 atm. For both (^{iPr}BPDI)V(NPh)(HNPh) and (^{iPr}BPDI)V(HNPh)$_2$, the calculated N−H BDFEs of 69.2 and 64.1 kcal/mol, respectively, are in agreement with the range established experimentally.

Based on the experimentally and computationally determined BDFEs, HAT between the bis(imido) and bis(anilido) complexes is thermodynamically favorable. To support these data, a crossover experiment between (^{iPr}BPDI)V(HNTol)$_2$ and (^{iPr}BPDI)V(NPh)$_2$ was conducted. While no reaction occurred at room temperature, slow formation of both (^{iPr}BPDI)V(NPh)(HNPh) and (^{iPr}BPDI)V(NTol)(HNTol) was observed upon heating to 80 °C for 3 days. Importantly, no scrambling of the ligand substituents was observed, supporting a simple HAT mechanism. The slow rate of HAT is not surprising considering the steric protection around the imido and anilido ligands imparted by the bulky 2,6-di-isopropylphenyl substituents of the supporting bis(imino)-pyridine ligand.

The BDFEs determined in this study are significantly lower than those of N−H bonds previously reported for middle and late transition metal amido complexes.[6] One of the most accurate determinations of an N−H BDFE in these systems was reported by Smith et al. for [(L^{Mes})Fe($HN^{t}Ad$)]$^+$ (L^{Mes} = phenyltris(1-mesitylimidazol-2-ylidene)borate) and yielded a value of 88 ± 5 kcal/mol.[6b] In agreement with this value, a number of late metal imido complexes undergo clean hydrogen atom abstraction from 1,4-cyclohexadiene (BDFE(C−H) ∼ 77 kcal/mol) or DHA and show reactivity toward hydrocarbon substrates with significantly stronger bonds (85−90 kcal/mol). These results highlight a general trend in transition metal imido/amido systems and emphasize different challenges in early versus late transition metal chemistry: High-valent early transition metals with low d electron counts can be accessed via N−N bond cleavage and form strong M−N multiple bonds, resulting in weak N−H bonds in their corresponding amido complexes. Consequently, imido complexes are readily available, but N−H bond formation is challenging. Moving toward later transition metals, the increasing d electron count results in occupation of M−N antibonding orbitals, weakening the M−N multiple bond. As a result, the reactivity of the imido species is increased and amido formation by hydrogen atom abstraction forming strong N−H bonds is preferred. The major challenge in late metal chemistry is, therefore, the generation of the high-valent imido species, which generally requires the use of strong oxidants such as iminoiodinanes or organic azides.

Mechanistic Insights into N−N Bond Cleavage and Hydrogen Atom Transfer Involving Hydrazine. The formation of (^{iPr}BPDI)V(HNPh)$_2$ from net oxidative addition of 1,2-diphenylhydrazine prompted further investigations into the mechanism of this transformation. Despite the weak N−N single bond in hydrazine,[21] direct oxidative addition to low-valent metal centers is perhaps surprisingly rare. The first example for this reaction was reported in 2007 by Mayer et al. with a tetranuclear precursor, (Cp*RuCl)$_4$, to generate the dinuclear complex [Cp*RuCl(μ-NHPh)]$_2$ with two bridging anilido ligands derived from diphenylhydrazine.[22] To establish that both anilido ligands in (^{iPr}BPDI)V(HNPh)$_2$ originate from the same hydrazine molecule, a 1:1 mixture of 1,2-diphenylhydrazine and 1,2-di(*p*-tolyl)hydrazine was added to a benzene-d_6 solution of [{(^{iPr}BPDI)V(THF)}$_2$(μ_2-N_2)]. Analysis of the outcome of the reaction was complicated by the paramagnetism and the lack of assignable NMR data for both the vanadium starting material and the corresponding products. Determination of the product ratio by EPR spectroscopy was precluded by the very similar EPR parameters of both the phenyl and tolyl

dx.doi.org/10.1021/ja5062196 | J. Am. Chem. Soc. 2014, 136, 12099−12107

derivatives (vide supra). To circumvent this problem and obtain products observable by NMR spectroscopy, a stoichiometric amount of TEMPO was added at the completion of the reaction. As described above, the TEMPO radical is capable of rapidly abstracting a single hydrogen atom from the paramagnetic bis(anilido) complex to cleanly generate diamagnetic ($^{i\mathrm{Pr}}$BPDI)V(N*Ar*)(NH*Ar*). Due to the very different time scales of the two reaction steps, the ratio of the initial hydrazine cleavage products should be unperturbed. The ^{1}H NMR spectrum of the product mixture exhibits two peaks at 10.11 and 10.41 ppm, which were assigned to the N−H protons of ($^{i\mathrm{Pr}}$BPDI)V(NPh)(HNPh) and ($^{i\mathrm{Pr}}$BPDI)V(NTol)(HNTol), respectively. These assignments were supported by independently prepared samples from control experiments where only a single hydrazine derivative was added. Upon closer inspection, however, each peak displays a small shoulder indicating trace amounts of additional vanadium products. In addition to the vanadium species, small amounts of *p*-toluidine and *p*-azotoluene were detected by the characteristic resonances of their methyl substituents, indicating an additional background reaction.

Similar results were obtained when heating [{($^{i\mathrm{Pr}}$BPDI)V(THF)}$_2$(μ_2-N$_2$)] in the presence of excess 1,2-diphenylhydrazine and 1,2-di(*p*-tolyl)hydrazine (1:1 ratio). As mentioned previously, ($^{i\mathrm{Pr}}$BPDI)V(N*Ar*)(NH*Ar*) complexes are the major products under these reaction conditions. In this experiment, four distinct N−H signals in approximately 1:3:3:2 ratio were identified between 10.0 and 10.5 ppm in the benzene-d_6 ^{1}H NMR spectrum (Figure 5). The main signals

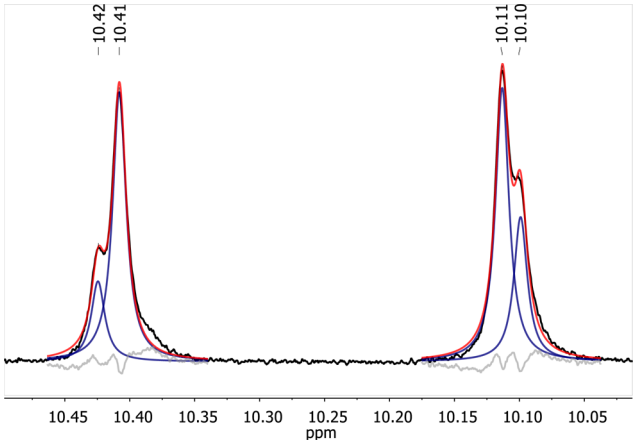

Figure 5. N−H region of the ^{1}H NMR spectrum for the reaction of a 1:1 mixture of 1,2-diphenylhydrazine and 1,2-di(*p*-tolyl)hydrazine with [{($^{i\mathrm{Pr}}$BPDI)V(THF)}$_2$(μ_2-N$_2$)]. The red line represents a fit of the data, and the blue lines shows the deconvolution of the individual peaks.

at 10.11 and 10.41 ppm were assigned as the homosubstituted products, while the remaining smaller signals at 10.10 and 10.42 ppm were tentatively assigned to the heterosubstituted compounds ($^{i\mathrm{Pr}}$BPDI)V(NTol)(HNPh) and ($^{i\mathrm{Pr}}$BPDI)V(NPh)(HNTol), respectively. The increased amount of heterosubstituted products under these conditions compared to the room temperature experiment followed by addition of TEMPO suggests that these compounds are the result of a side reaction rather than from the initial formation of the bis(anilido) vanadium complexes.

Additionally, complete conversion of the hydrazines with concomitant formation of aniline, *p*-toluidine, azobenzene, and *p*-azotoluene was observed, indicating competing disproportionation of the 1,2-diarylhydrazines. These results raised further questions about the mechanism of formation of ($^{i\mathrm{Pr}}$BPDI)V(N*Ar*)(NH*Ar*) complexes from the reaction of [{($^{i\mathrm{Pr}}$BPDI)V(THF)}$_2$(μ_2-N$_2$)] with 1,2-diarylhydrazines as well as the origin of hydrazine disproportionation. To address these questions, the reactivity of 1,2-diarylhydrazines toward isolated samples of the vanadium bis(imido), imido/anilido, and bis(anilido) complexes was explored. As shown above, ($^{i\mathrm{Pr}}$BPDI)V(NPh)$_2$ undergoes rapid HAT with 1,2-diphenylhydrazine to generate the mixed imido/anilido complex. Similarly, the reaction with 1,2-di(*p*-tolyl)hydrazine resulted in clean conversion to ($^{i\mathrm{Pr}}$BPDI)V(NPh)(HNPh) and 0.5 equiv of *p*-azotoluene without scrambling of the ligand substituents.

Addition of 10 equiv of 1,2-di(*p*-tolyl)hydrazine to ($^{i\mathrm{Pr}}$BPDI)V(NPh)(HNPh) at room temperature resulted in very slow disproportionation of the hydrazine. Even upon heating to 80 °C, the reaction requires multiple days for complete conversion. Notably, no incorporation of tolyl substituents into the vanadium compound was detected based on the N−H signals as well as the *p*-tolyl methyl signals in the ^{1}H NMR spectrum of the product mixture. Reassuringly, no aniline is formed during the reaction, while *p*-toluidine and *p*-azotoluene are formed in the expected 2:1 ratio. These experiments clearly show that imido/anilido bis(imino)pyridine vanadium complexes are competent precatalysts for the disproportionation of 1,2-diarylhydrazines. We note that formation of the ($^{i\mathrm{Pr}}$BPDI)V(NPh)(HNPh) from the corresponding vanadium dinitrogen compound occurs within 72 h, while the time scale of hydrazine disproportionation is slow, owing in part to the necessity of forming ($^{i\mathrm{Pr}}$BPDI)V(NPh)(HNPh).

Finally, an isolated sample of ($^{i\mathrm{Pr}}$BPDI)V(HNTol)$_2$ was subjected to excess 1,2-diphenylhydrazine. Only small amounts of imido/anilido products were detected after 24 h at room temperature. Heating to 80 °C resulted in slow formation of two imido/anilido products identified as ($^{i\mathrm{Pr}}$BPDI)V(NTol)(HNPh) and ($^{i\mathrm{Pr}}$BPDI)V(NTol)(HNTol) based on the N−H signals in the ^{1}H NMR spectrum. Importantly, the homosubstituted complex is formed as the major product, in agreement with the initial crossover experiment of [{($^{i\mathrm{Pr}}$BPDI)V(THF)}$_2$(μ_2-N$_2$)] with 1,2-diarylhydrazines.

A summary of the observed reactivity of 1,2-diarylhydrazines toward bis(imino)pyridine vanadium complexes is shown in Scheme 2. Importantly, the presented crossover experiments using 1,2-diphenyl- and 1,2-di(*p*-tolyl)hydrazine establish that exchange of anilido ligands occurs only upon reaction of ($^{i\mathrm{Pr}}$BPDI)V(NH*Ar*)$_2$ with diarylhydrazines to yield ($^{i\mathrm{Pr}}$BPDI)V(N*Ar*)(NH*Ar*). No exchange of imido ligands was observed.

The disproportionation of 1,2-diarylhydrazines has been observed previously in several multinuclear[22,23] and mononuclear[24] systems with transition metal and actinide catalysts. For the mononuclear catalysts, HAT involving metal imido intermediates has been proposed as a key step of the catalytic cycle. On the basis of these studies and the experimental and computational results presented here, we propose the catalytic cycle shown in Scheme 3 for the disproportionation of 1,2-diarylhydrazines catalyzed by ($^{i\mathrm{Pr}}$BPDI)V(NPh)(HNPh). Initial HAT from the anilido ligand to hydrazine with concomitant N−N bond cleavage furnishes the bis(imido) complex, ($^{i\mathrm{Pr}}$BPDI)V(NPh)$_2$, the first equivalent of aniline and an anilide

dx.doi.org/10.1021/ja5062196 | J. Am. Chem. Soc. 2014, 136, 12099−12107

Scheme 2. Reactivity of Bis(imino)pyridine Vanadium Complexes with Azoarenes and 1,2-Diarylhydrazines

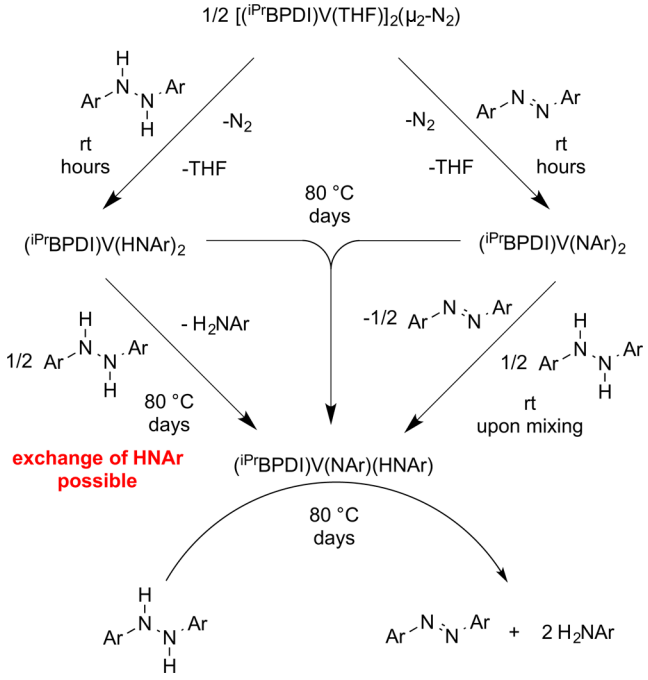

Scheme 3. Proposed Mechanism for the Vanadium-Catalyzed Disproportionation of 1,2-Diphenylhydrazine

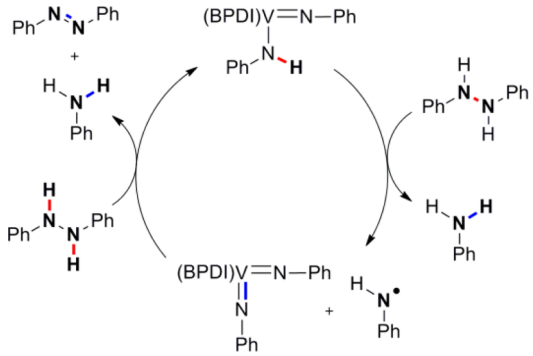

radical. DFT calculations were performed to estimate the free energy for the addition of a single hydrogen atom to 1,2-diphenylhydrazine with concomitant N−N bond cleavage and furnished a value of −67.2 kcal/mol. If we assume the computed and experimentally supported value of 69.2 kcal/mol for the BDFE of the N−H bond in (^{iPr}BPDI)V(NPh)(HNPh), this HAT is only slightly energetically increased by 2 kcal/mol and should be accessible at 80 °C. This is further supported by the report that the organic hydrogen atom donor DHA, with a significantly higher BDFE(C−H) of 76.0 kcal/mol, is competent for the reduction of azobenzene and 1,2-diphenylhydrazine to aniline via a HAT mechanism albeit at higher temperatures (>250 °C).[25] An alternative pathway, in which a hydrogen atom is transferred from the hydrazine to (^{iPr}BPDI)V(NPh)(HNPh) to yield the bis(anilido) complex (^{iPr}BPDI)V(HNPh)$_2$, can be ruled out as ligand exchange would be expected under these conditions but was not observed during the disproportionation reaction (vide supra).

Following the initial HAT, the anilide radical can abstract a hydrogen atom from 1,2-diphenylhydrazine to generate a second equivalent of aniline (BDFE(N−H) in aniline: exptl 90.1 kcal/mol,[20] DFT 86.8 kcal/mol) while the bis(imido) complex abstracts the second hydrogen atom to furnish azobenzene and regenerate (^{iPr}BPDI)V(NPh)(HNPh). Alternatively, the anilide radical is capable of abstracting a hydrogen atom from a second imido/amido complex to generate a second equivalent of both aniline and (^{iPr}BPDI)V(NPh)$_2$. Facile HAT between the bis(imido) complex and 1,2-diphenylhydrazine furnishes 1 equiv of azobenzene and regenerates (^{iPr}BPDI)V(NPh)(HNPh) to complete the catalytic cycle.

CONCLUDING REMARKS

Understanding N−H bond formation and N−N bond cleavage reactions is of paramount importance to the development of molecular catalysts for N_2 functionalization. Herein we have shown that the reaction of the bis(imino)pyridine vanadium dinitrogen complex [{(^{iPr}BPDI)V(THF)}$_2$(μ_2-N_2)] with 1,2-diarylhydrazines resulted in the rare net oxidative addition of the N−N single bond to a single vanadium center and formation of (^{iPr}BPDI)V(NH*Ar*)$_2$. Crossover experiments with hydrazines bearing different arene substituents established that both anilido ligands originate from the same hydrazine molecule, in agreement with direct N−N oxidative addition. Combined experimental and theoretical analyses of the electronic structure of the product established that the metal center maintains a +III oxidation state, while the reducing equivalents for the N−N bond cleavage are supplied by the pincer ligand and the bridging N_2^{2-} unit, highlighting the utility of redox-active ligands as a scaffold for multielectron bond cleavage reactions. The reaction of the vanadium bis(anilido) complex with excess 1,2-diphenylhydrazine or hydrogen atom acceptors led to the isolation and characterization of the mixed imido/anilido complex (^{iPr}BPDI)V(NPh)(HNPh). Alternatively, this complex was readily accessible via HAT to the previously reported bis(imino)pyridine vanadium bis(imido) complex (^{iPr}BPDI)V(NPh)$_2$. The triad of crystallographically characterized bis-imido, imido/anilido, and bis-anilido complexes allowed the experimental and computational determination of N−H bond dissociation free energies for compounds derived directly from N−N bond cleavage. The N−H BDFE was drastically influenced by the oxidation state of both the metal and the redox-active bis(imino)pyridine where stronger N−H bonds of 69.2 kcal/mol were determined for a vanadium(V) compound with a two-electron reduced chelate. Reduction of the oxidation state of the metal to V(III) with concomitant one-electron oxidation of the chelate resulted in a significant decrease in the N−H BDFE to 64.1 kcal/mol, likely a consequence of diminished vanadium−nitrogen multiple bond character. These studies highlight the electronic flexibility of the bis(imino)pyridine framework and how its readily accessible redox states enable the metal to finely adjust to the changing ligand environment and alter homolytic N−H bond strengths. Notably, trends opposite those expected for Werner-type compounds are observed, where lower oxidation states and hence higher d counts typically result in stronger N−H bonds due to diminished π-bonding in the product. The redox-active ligand allows the vanadium to maintain a high oxidation state and hence V−N π-bonding upon hydrogen atom abstraction, inverting the expected N−H BDFEs. Such insights into bonding and associated thermodynamics should prove valuable in the development of synthetic schemes for the reduction of N_2 and its hydrogenated products.

dx.doi.org/10.1021/ja5062196 | J. Am. Chem. Soc. 2014, 136, 12099−12107

EXPERIMENTAL SECTION

General Considerations. All air- and moisture-sensitive manipulations were carried out using standard high vacuum line, Schlenk, or cannula techniques or in an MBraun inert atmosphere drybox containing an atmosphere of purified nitrogen. The MBraun drybox was equipped with a cold well designed for freezing samples in liquid nitrogen. Solvents for air- and moisture-sensitive manipulations were dried and deoxygenated using literature procedures.[26] Deuterated solvents for NMR spectroscopy were distilled from sodium metal under an atmosphere of argon and stored over 4 Å molecular sieves. 1,2-Di(*p*-tolyl)hydrazine[27] and anhydrous TEMPO-H[28] were prepared following literature procedures. TEMPO and 1,2-diphenylhydrazine were purchased from Sigma-Aldrich. 1,2-Diphenylhydrazine was recrystallized from diethyl ether/pentane solution prior to use to remove trace amounts of azobenzene.

^{1}H NMR spectra were recorded on a Varian Inova 400 spectrometer operating at 399.860 MHz. All chemical shifts are reported relative to $SiMe_4$ using ^{1}H (residual) chemical shifts of the solvent as a secondary standard. ^{13}C NMR spectra were recorded on a Bruker 500 spectrometer operating at 125.71 MHz. ^{13}C chemical shifts are reported relative to $SiMe_4$ using chemical shifts of the solvent as a secondary standard where applicable. Infrared spectroscopy was conducted on a Thermo-Nicolet iS10 FT-IR spectrometer calibrated with a polystyrene standard. Elemental analyses were performed at Robertson Microlit Laboratories, Inc., in Ledgewood, NJ. Gouy magnetic susceptibility balance measurements were performed with a Johnson Matthey instrument that was calibrated with $HgCo(SCN)_4$. Continuous wave EPR spectra were recorded at room temperature on an X-band Bruker EMXPlus spectrometer equipped with an EMX standard resonator and a Bruker PremiumX microwave bridge. The spectra were simulated using EasySpin for MATLAB.[29] Single crystals suitable for X-ray diffraction were coated with polyisobutylene oil in a drybox, transferred to a nylon loop, and then quickly transferred to the goniometer head of a Bruker X8 APEX2 diffractometer equipped with molybdenum and copper X-ray tubes (λ = 0.71073 and 1.54184 Å, respectively). Preliminary data revealed the crystal system. The data collection strategy was optimized for completeness and redundancy using the Bruker COSMO software suite. The space group was identified, and the data were processed using the Bruker SAINT+ program and corrected for absorption using SADABS. The structures were solved using direct methods (SHELXS) completed by subsequent Fourier synthesis and refined by full-matrix least-squares procedures.

Quantum-Chemical Calculations. All DFT calculations were performed with the ORCA program package in the gas phase.[30] The geometry optimizations of the complexes and single-point calculations on the optimized geometries were carried out at the B3LYP level of DFT.[31] The all-electron Gaussian basis sets were those developed by the Ahlrichs group.[32] Triple-ζ quality basis sets def2-TZVP with one set of polarization functions on vanadium and on the atoms directly coordinated to the metal center were used. For the carbon and hydrogen atoms, slightly smaller polarized split-valence def2-SV(P) basis sets were used that were of double-ζ quality in the valence region and contained a polarizing set of d functions on the non-hydrogen atoms. Auxiliary basis sets to expand the electron density in the resolution-of-the-identity (RIJCOSX)[33] approach were chosen to match the orbital basis.[34] Numerical frequencies were calculated at the same level of theory to confirm the optimized geometries (no imaginary frequencies) and to derive thermochemical data. Bond dissociation free energies were computed at standard conditions of 1 atm and 298 K including corrections for vibrational zero-point energy, as well as contributions from translational, rotational, and vibrational modes to the energy and entropy of the homolytic bond cleavage process. For the calculation of EPR parameters, the "core properties" basis set developed by Neese[35] was used for vanadium, and the IGLO-III[36] basis set was used for nitrogen and hydrogen. Throughout this paper, we describe our computational results by using the broken-symmetry (BS) approach by Ginsberg and Noodleman. Because several broken symmetry solutions to the spin-unrestricted Kohn–Sham equations may be obtained, the general notation BS(m,n) has been adopted, where m(n) denotes the number of spin-up (spin-down) electrons at the two interacting fragments. All spin density plots were generated with the program Molekel.[37]

Preparation of (^{iPr}BPDI)V(HNTol)$_2$. A solution of 29 mg (137 μmol) of 1,2-di(*p*-tolyl)hydrazine in 2 mL of diethyl ether was added to a solution of 100 mg (67 μmol) of [(^{iPr}BPDI)V(THF)]$_2$(μ_2-N$_2$) in 10 mL of diethyl ether. The resulting mixture was stirred for 5 h, during which the color of the solution changed from dark green to dark red. The solvent was removed in vacuum, and the dark red residue was redissolved in a minimum amount of pentane and cooled to −35 °C, yielding 68 mg (58%) of a red solid identified as (^{iPr}BPDI)V(HNtol)$_2$. Single crystals suitable for X-ray diffraction were obtained by cooling a concentrated solution of the product in pentane/toluene (20:1) to −35 °C. Anal. Calcd for $C_{57}H_{63}N_5V$: C, 78.77; H, 7.31; N, 8.06. Found: C, 78.56; H, 7.39; N, 7.84.

Preparation of (^{iPr}BPDI)V(HNPh)$_2$. This compound was prepared analogous to (^{iPr}BPDI)V(HNTol)$_2$ using stoichiometric amounts of 1,2-diphenylhydrazine. Yield 75 mg (67%). Anal. Calcd for $C_{55}H_{59}N_5V$: C, 78.54; H, 7.07; N, 8.33. Found: C, 78.75; H, 6.70; N, 8.72.

Preparation of (^{iPr}BPDI)V(NPh)(HNPh). A solution of 19 mg (121 μmol) of TEMPO-H in 2 mL of diethyl ether was added to a solution of 100 mg (119 μmol) of (^{iPr}BPDI)V(NPh)$_2$ in 8 mL of diethyl ether, and the resulting mixture was stirred for 15 min. The solvent was removed in vacuum, and the dark brown residue was redissolved in a minimum amount of diethyl ether, layered with approximately 5 mL of bis(trimethylsilyl)ether, and cooled to −35 °C, yielding 41 mg (41%) of brown crystals identified as (^{iPr}BPDI)V(NPh)(HNPh). Anal. Calcd for $C_{55}H_{58}N_5V$: C, 78.64; H, 6.96; N, 8.34. Found: C, 78.35; H, 6.51; N, 7.99. ^{1}H NMR (benzene-d_6): δ 0.28 (d, 6H, $^3J_{HH}$ = 6.6 Hz, *i*Pr-CH$_3$), 0.97 (d, 6H, $^3J_{HH}$ = 6.5 Hz, *i*Pr-CH$_3$), 1.03 (d, 6H, $^3J_{HH}$ = 6.7 Hz, *i*Pr-CH$_3$), 1.42 (d, 6H, $^3J_{HH}$ = 6.6 Hz, *i*Pr-CH$_3$), 2.40 (septet, 2 H, $^3J_{HH}$ = 6.7 Hz, *i*Pr-CH), 3.70 (septet, 2 H, $^3J_{HH}$ = 6.7 Hz, *i*Pr-CH), 5.76 (d, 2 H, $^3J_{HH}$ = 8.0 Hz, ArH), 6.34 (t, 1 H, $^3J_{HH}$ = 7.6 Hz, ArH), 6.72 (t, 1 H, $^3J_{HH}$ = 7.3 Hz, ArH), 6.80−7.01 (m, 15 H, ArH), 7.19−7.31 (m, 10 H, ArH), 10.11 (s, 1 H, NH). ^{13}C NMR (benzene-d_6): δ 22.41 (*i*Pr-CH$_3$), 24.28 (*i*Pr-CH$_3$), 24.64 (*i*Pr-CH$_3$), 25.63 (*i*Pr-CH$_3$), 27.29 (*i*Pr-CH), 29.48 (*i*Pr-CH), 120.27 (Ar-CH), 121.37 (Ar-CH), 122.30 (Ar-CH), 122.63 (Ar-CH), 123.78 (Ar-CH), 124.65 (Ar-CH), 125.42 (Ar-CH), 126.98 (Ar-CH), 127.97 (Ar-CH), 128.16 (Ar-CH), 128.35 (Ar-CH), 129.09 (Ar-CH), 129.13 (Ar-CH), 133.50 (Ar-C), 137.33 (Ar-C), 141.53 (Ar-C), 142.71 (Ar-C), 152.04 (Ar-C), 157.14 (Ar-C), 160.43 (Ar-C), 161.92 (C═NAr).

ASSOCIATED CONTENT

Supporting Information

Additional experimental procedures, spectroscopic and computational data. Crystallographic data for (^{iPr}BPDI)V(HNTol)$_2$ and (^{iPr}BPDI)V(NPh)(HNPh) in cif format. This material is available free of charge via the Internet at http://pubs.acs.org.

AUTHOR INFORMATION

Corresponding Author

pchirik@princeton.edu

Notes

The authors declare no competing financial interest.

ACKNOWLEDGMENTS

We thank the Air Force Office for Scientific Research (FA9550-11-10252) for financial support.

REFERENCES

(1) (a) Hoffman, B. M.; Dean, D. R.; Seefeldt, L. C. *Acc. Chem. Res.* **2009**, *42*, 609. (b) Burgess, B. K.; Lowe, D. L. *Chem. Rev.* **1996**, *96*, 2983. (c) Thorneley, R. N. F.; Lowe, D. J. In *Molybdenum Enzymes*;

Spiro, T. G., Ed.; Wiley-Interscience: New York, 1985; Vol. 7; pp 89–116.
(2) (a) Yandulov, D. V.; Schrock, R. R. *Science* **2003**, *301*, 76. (b) Arashiba, K.; Miyake, Y.; Nishibayashi, Y. *Nat. Chem.* **2011**, *3*, 120. (c) Schrock, R. R. *Acc. Chem. Res.* **2005**, *38*, 955. (d) Anderson, J. S.; Rittle, J.; Peters, J. C. *Nature* **2013**, *501*, 7465.
(3) van der Ham, C. J. M.; Koper, M. T. M.; Hetterscheid, D. G. H. *Chem. Soc. Rev.* **2014**, *43*, 5183.
(4) (a) Jensen, M. P.; Mehn, M. P.; Que, L., Jr. *Angew. Chem., Int. Ed.* **2003**, *42*, 4357. (b) Thyagarajan, S.; Shay, D. T.; Incarvito, C. D.; Rheingold, A. L.; Theopold, K. H. *J. Am. Chem. Soc.* **2003**, *125*, 4440. (c) Shay, D. T.; Yap, G. P. A.; Zakharov, L. N.; Rheingold, A. L.; Theopold, K. H. *Angew. Chem., Int. Ed.* **2005**, *44*, 1508. (d) Lucas, R. L.; Powell, D. R.; Borovik, A. S. *J. Am. Chem. Soc.* **2005**, *127*, 11596. (e) Badiei, Y. M.; Dinescu, A.; Dai, X.; Palomino, R. M.; Heinemann, F. W.; Cundari, T. R.; Warren, T. H. *Angew. Chem., Int. Ed.* **2008**, *47*, 9961. (f) Ni, C.; Fettinger, J. C.; Long, G. J.; Brynda, M.; Power, P. P. *Chem. Commun.* **2008**, 6045. (g) Avenier, F.; Gouré, E.; Dubourdeaux, P.; Sénèque, O.; Oddou, J.-L.; Pécaut, J.; Chardon-Noblat, S.; Deronzier, A.; Latour, J.-M. *Angew. Chem., Int. Ed.* **2008**, *47*, 715. (h) Chomitz, W. A.; Arnold, J. *Chem. Commun.* **2008**, 3648. (i) King, E. R.; Betley, T. A. *Inorg. Chem.* **2009**, *48*, 2361. (j) Fantauzzi, S.; Gallo, E.; Caselli, A.; Ragaini, F.; Casati, N.; Macchi, P.; Cenini, S. *Chem. Commun.* **2009**, 3952. (k) Mankad, N. P.; Müller, P.; Peters, J. C. *J. Am. Chem. Soc.* **2010**, *132*, 4083.
(5) (a) Kogut, E.; Wiencko, H. L.; Zhang, L.; Cordeau, D. E.; Warren, T. H. *J. Am. Chem. Soc.* **2005**, *127*, 11248. (b) Wiese, S.; McAfee, J. L.; Pahls, D. R.; McMullin, C. L.; Cundari, T. R.; Warren, T. H. *J. Am. Chem. Soc.* **2012**, *134*, 10114. (c) Cowley, R. E.; Holland, P. L. *Inorg. Chem.* **2012**, *51*, 8352.
(6) (a) Cowley, R. E.; Bontchev, R. P.; Sorrell, J.; Sarracino, O.; Feng, Y.; Wang, H.; Smith, J. M. *J. Am. Chem. Soc.* **2007**, *129*, 2424. (b) Nieto, I.; Ding, F.; Bontchev, R. P.; Wang, H.; Smith, J. M. *J. Am. Chem. Soc.* **2008**, *130*, 2716.
(7) (a) Iluc, V. M.; Hillhouse, G. L. *J. Am. Chem. Soc.* **2010**, *132*, 15148. (b) Iluc, V. M.; Miller, A. J. M.; Anderson, J. S.; Monreal, M. J.; Mehn, M. P.; Hillhouse, G. L. *J. Am. Chem. Soc.* **2011**, *133*, 13055.
(8) Berry, J. F. *Comments Inorg. Chem.* **2009**, *30*, 28.
(9) (a) Kornecki, K. P.; Berry, J. F. *Chem.—Eur. J.* **2011**, *17*, 5827. (b) Lyaskovskyy, V.; Olivos Suarez, A. I.; Lu, H.; Jiang, H.; Zhang, X. P.; de Bruin, B. J. *Am. Chem. Soc.* **2011**, *133*, 12264. (c) Wiese, S.; McAfee, J. L.; Pahls, D. R.; McMullin, C. L.; Cundari, T. R.; Warren, T. H. *J. Am. Chem. Soc.* **2012**, *134*, 10114. (d) King, E. R.; Hennessy, E. T.; Betley, T. A. *J. Am. Chem. Soc.* **2011**, *133*, 4917. (e) Hennessy, E. T.; Betley, T. A. *Science* **2013**, *340*, 591.
(10) (a) Fryzuk, M. D.; Johnson, S. A. *Coord. Chem. Rev.* **2000**, *200–202*, 379. (b) MacKay, B. A.; Fryzuk, M. D. *Chem. Rev.* **2004**, *104*, 385. (c) Shaver, M. P.; Fryzuk, M. D. *Adv. Synth. Catal.* **2003**, *345*, 1061.
(11) (a) Nugent, W. A.; Mayer, J. M. *Metal-Ligand Multiple Bonds*; John Wiley & Sons: New York, 1988. (b) Eikey, R. A.; Abu-Omar, M. M. *Coord. Chem. Rev.* **2003**, *243*, 83.
(12) For examples of N–H bond formation by 1,2-addition including to coordinated dinitrogen, see: (a) Schaller, C. P.; Cummins, C. C.; Wolczanski, P. T. *J. Am. Chem. Soc.* **1996**, *118*, 591. (b) Hoyt, H. M.; Michael, F. E.; Bergman, R. G. *J. Am. Chem. Soc.* **2004**, *126*, 1018. (c) Bernskoetter, W. H.; Lobkovsky, E.; Chirik, P. J. *J. Am. Chem. Soc.* **2005**, *40*, 14051. (d) Pool, J. A.; Bernskoetter, W. H.; Chirik, P. J. *J. Am. Chem. Soc.* **2004**, *126*, 14326.
(13) Chirik, P. J.; Wieghardt, K. *Science* **2010**, *327*, 794.
(14) Milsmann, C.; Turner, Z. R.; Semproni, S. P.; Chirik, P. J. *Angew. Chem., Int. Ed.* **2012**, *51*, 5386.
(15) Bart, S. C.; Lobkovsky, E.; Bill, E.; Chirik, P. J. *J. Am. Chem. Soc.* **2006**, *128*, 5302.
(16) Bowman, A. C.; Milsmann, C.; Bill, E.; Turner, Z. R.; Lobkovsky, E.; DeBeer, S.; Wieghardt, K.; Chirik, P. J. *J. Am. Chem. Soc.* **2011**, *133*, 17353.
(17) Heyduk, A. F.; Zarkesh, R. A.; Nguyen, A. I. *Inorg. Chem.* **2011**, *50*, 9849.
(18) (a) de Bruin, B.; Bill, E.; Bothe, E.; Weyhermüller, T.; Wieghardt, K. *Inorg. Chem.* **2000**, *39*, 2936. (b) Budzelaar, P. H. M.; de Bruin, B.; Gal, A. W.; Wieghardt, K.; van Lenthe, J. H. *Inorg. Chem.* **2001**, *40*, 4649. (c) Knijnenburg, Q.; Gambarotta, S.; Budzelaar, P. H. M. *Dalton Trans.* **2006**, 5442. (d) Bart, S. C.; Chlopek, K.; Bill, E.; Bouwkamp, M. W.; Lobkovsky, E.; Neese, F.; Wieghardt, K.; Chirik, P. J. *J. Am. Chem. Soc.* **2006**, *128*, 13901.
(19) Vidyaratne, I.; Gambarotta, S.; Korobkov, I.; Budzelaar, P. H. M. *Inorg. Chem.* **2005**, *44*, 1187.
(20) Warren, J. J.; Tronic, T. A.; Mayer, J. M. *Chem. Rev.* **2010**, *110*, 6961.
(21) Cole, L. G.; Gilbert, E. C. *J. Am. Chem. Soc.* **1951**, *73*, 5423.
(22) Hoover, J. M.; DiPasquale, A.; Mayer, J. M.; Michael, F. E. *Organometallics* **2007**, *26*, 3297.
(23) (a) Kuwata, S.; Mizobe, Y.; Hidai, M. *Inorg. Chem.* **1994**, *33*, 3619. (b) Hitchcock, P. B.; Hughes, D. L.; Maguire, M. J.; Marjani, K.; Richards, R. L. *J. Chem. Soc., Dalton Trans.* **1997**, 4747. (c) Takei, I.; Dohki, K.; Kobayashi, K.; Suzuki, T.; Hidai, M. *Inorg. Chem.* **2005**, *44*, 3768.
(24) (a) Peters, R. G.; Warner, B. P.; Burns, C. J. *J. Am. Chem. Soc.* **1999**, *121*, 5585. (b) Blackmore, K. J.; Lal, N.; Ziller, J. W.; Heyduk, A. F. *J. Am. Chem. Soc.* **2008**, *130*, 2728.
(25) Coellen, M.; Rüchardt, C. *Chem.—Eur. J.* **1995**, *1*, 564.
(26) Pangborn, A. B.; Giardello, M. A.; Grubbs, R. H.; Rosen, R. K.; Timmers, F. J. *Organometallics* **1996**, *15*, 1518.
(27) Sakai, N.; Fujii, K.; Nabeshima, S.; Ikeda, R.; Konakahara, T. *Chem. Commun.* **2010**, *46*, 3173.
(28) Giffin, N. A.; Makramalla, M.; Hendsbee, A. D.; Robertson, K. N.; Sherren, C.; Pye, C. C.; Masuda, J. D.; Clyburne, J. A. C. *Org. Biomol. Chem.* **2011**, *9*, 3672.
(29) Stoll, S.; Schweiger, A. *J. Magn. Reson.* **2006**, *178*, 42.
(30) Neese, F. *Wiley Interdiscip. Rev.: Comput. Mol. Sci.* **2012**, *2*, 73.
(31) (a) Becke, A. D. J. *Chem. Phys.* **1986**, *84*, 4524. (b) Becke, A. D. J. *Chem. Phys.* **1993**, *98*, 5648. (c) Lee, C. T.; Yang, W. T.; Parr, R. G. *Phys. Rev. B* **1988**, *37*, 785.
(32) (a) Schäfer, A.; Horn, H.; Ahlrichs, R. J. *Chem. Phys.* **1992**, *97*, 2571. (b) Schäfer, A.; Huber, C.; Ahlrichs, R. *J. Chem. Phys.* **1994**, *100*, 5829. (c) Weigend, F.; Ahlrichs, R. *Phys. Chem. Chem. Phys.* **2005**, *7*, 3297.
(33) (a) Neese, F.; Wennmohs, F.; Hansen, A.; Becker, U. *Chem. Phys.* **2009**, *356*, 98. (b) Kossmann, S.; Neese, F. *Chem. Phys. Lett.* **2009**, *481*, 240. (c) Neese, F. J. *Comput. Chem.* **2003**, *24*, 1740.
(34) (a) Eichkorn, K.; Weigend, F.; Treutler, O.; Ahlrichs, R. *Theor. Chem. Acc.* **1997**, *97*, 119. (b) Eichkorn, K.; Treutler, O.; Öhm, H.; Häser, M.; Ahlrichs, R. *Chem. Phys. Lett.* **1995**, *240*, 283. (c) Eichkorn, K.; Treutler, O.; Öhm, H.; Häser, M.; Ahlrichs, R. *Chem. Phys. Lett.* **1995**, *242*, 652.
(35) The ORCA basis set "CoreProp" was used. This basis is based on the TurboMole DZ basis developed by Ahlrichs and co-workers and obtained from the basis set library under ftp.chemie.uni-karlsruhe.de/pub/basen.
(36) Kutzelnigg, W.; Fleischer, U.; Schindler, M. In *The IGLO-Method: Ab Initio Calculation and Interpretation of NMR Chemical Shifts and Magnetic Susceptibilities*; Springer-Verlag: Heidelberg, 1990; Vol. 23.
(37) *Molekel*, Advanced Interactive 3D-Graphics for Molecular Sciences, available under http://www.cscs.ch/molekel/.